Renyi entropies for classical string-net models

M. Hermanns and S. Trebst
Institute for Theoretical Physics of Cologne, 50937 Cologne, Germany
(Received 17 September 2013; revised manuscript received 16 April 2014; published 9 May 2014)

In quantum mechanics, string-net condensed states—a family of prototypical states exhibiting nontrivial topological order—can be classified via their long-range entanglement properties, in particular, topological corrections to the prevalent area law of the entanglement entropy. Here we consider classical analogs of such string-net models whose partition function is given by an equal-weight superposition of classical string-net configurations. Our analysis of the Shannon and Renyi entropies for a bipartition of a given system reveals that the prevalent volume law for these classical entropies is augmented by subleading topological corrections that are intimately linked to the anyonic theories underlying the construction of the classical models. We determine the universal values of these topological corrections for a number of underlying anyonic theories including $SU(2)_k$, $SU(N)_1$, and $SU(N)_2$ theories.

DOI: 10.1103/PhysRevB.89.205107 PACS number(s): 65.40.gd, 89.70.Cf, 05.20.−y

I. INTRODUCTION

The concept of topological order—long-range order beyond the conventional paradigm of symmetry broken order—has profoundly broadened our view of strongly correlated systems over the last decades [1]. Archetypal realizations of actual materials exhibiting such unconventional order include the (fractional) quantum Hall liquids [2] discovered over 30 years ago, Sr_2RuO_4 as a possible realization of a $p_x + ip_y$ superconductor [3] or in the more recent past the discovery of topological band insulators [4]. Further insight into the rich physics of topologically ordered systems has been achieved by the analytical understanding of exactly solvable spin models including the toric code [5] or Kitaev's honeycomb model [6].

Despite all this progress it has remained a challenging task to unambiguously identify a topologically ordered state in a given system—both in experiments or theoretical approaches. On the analytical side, concepts from quantum information theory have proven particularly helpful in generating a powerful measure of topological order in model systems. A key insight is that the topological order present in a quantum many-body system is reflected in its entanglement properties. In its most pronounced incarnation the long-range order present in topologically ordered systems leads to long-range entangled states [7], a scenario that applies to most of the examples of topologically ordered states above. The notable exception are the topological band insulators which exhibit short-range entanglement [8]. Here we will focus on the former class of long-range entangled states. A key concept to measure entanglement in a quantum many-body system is the entanglement entropy calculated by dividing the system into two parts A and B as illustrated in Fig. 1, obtaining the reduced density matrix of one partition by tracing out the other, e.g., $\hat{\rho}_A = \mathrm{Tr}_B(|\psi\rangle\langle\psi|)$, and then collapsing the information in the reduced density matrix into the so-called entanglement entropy

$$S_A = -\mathrm{Tr}_A[\hat{\rho}_A \ln \hat{\rho}_A]\,.$$

Despite the relatively broad-brush character of the entanglement entropy studying its dependence on the geometry of the bipartition has been shown to allow for a rather general classification of ground states of interacting quantum many-body systems. For systems restricted to two spatial dimensions, the entanglement entropy exhibits a so-called "area law" or more specifically a "boundary law" for all gapped ground states; it grows with the length ℓ of the boundary between the partitions A and B

$$S_A = c_\ell \ell - \gamma_{\mathrm{quantum}} + \cdots\,, \tag{1}$$

where any additional terms indicated by the dots are subleading terms of order $O(1/\ell)$, i.e., vanish in the limit $\ell \to \infty$. One of the more striking features of this boundary law is the occurrence of a subleading constant contribution that for a smooth boundary, i.e., one without any sharp corners, is independent of the size or the geometry of the bipartition and thus indicates long-range entanglement. This constant $\gamma_{\mathrm{quantum}}$ is often called the *topological entropy* [9,10], since it strictly vanishes for disordered or conventionally ordered states while for a topologically ordered state it always remains finite. In fact, the topological entropy has to lock into a universal value, which is tightly connected to the effective topological field theory describing the nonlocal topological order in the system at hand. It was shown [9,10] that

$$\gamma_{\mathrm{quantum}} = \ln\, \mathcal{D}, \tag{2}$$

where $\mathcal{D}$ is the so-called total quantum dimension, an important characteristic of the effective topological field theory. The same is true for the topological entropy of the Renyi entropies $S_n = \frac{1}{1-n}\mathrm{Tr}_A[\hat{\rho}_A^n]$—a generalization of the entanglement entropy that is often easier to compute [11]. An alternative perspective to understand the origin of a finite constant $\gamma_{\mathrm{quantum}}$ for a topologically ordered state emerges from considering the entropic contribution arising solely from the boundary. In contrast to a conventionally ordered or entirely disordered system, the states on the boundary of a topologically ordered system are found to be subtly constrained which then leads to a nontrivial entropic contribution of this boundary. We will discuss details of both perspectives in the remainder of the manuscript.

Despite the obvious fact that classical systems do not exhibit any entanglement, the notion of the entanglement entropy has a straightforward companion for classical statistical systems—the Shannon entropy, which we can analogously define for a

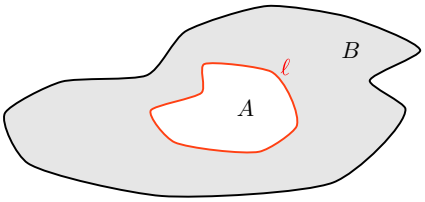

FIG. 1. (Color online) Bipartition of a quantum system.

bipartition of the system as illustrated in Fig. 1. It is then given as

$$S_A = -\sum_{\{j_A\}} p_{j_A} \ln p_{j_A} , \tag{3}$$

where $\{j_A\}$ denotes the set of possible classical configurations in A and p_{j_A} is the statistical probability of a given configuration j_A.

The analogy to the entanglement entropy goes even one step further, as the Shannon entropy also exhibits a rather characteristic scaling with the size and the geometry of the bipartition. In its most general form it follows a "volume law" of the form

$$S_A = c_V V_A + c_\ell \ell - \gamma_{\text{classical}} + \cdots , \tag{4}$$

where V_A is the volume of partition A and ℓ is again the length of the boundary of the partition. The dots indicate subleading terms that vanish in the limit of $V_A, \ell \to \infty$.

The occurrence of a nonvanishing constant term $\gamma_{\text{classical}}$ in this volume law for the classical Shannon entropy is again tightly connected to the occurrence of long-range information in the classical system. A prototypical family of such classical systems exhibiting long-range information are classical variants of so-called string-net states, which we will introduce and discuss in much detail in the following. The main result of this manuscript is that for this broad variety of classical systems we establish a universal equation relating the constant term $\gamma_{\text{classical}}$ to a characteristic feature of the topological field theory underlying these string-net states. The methods that allow us to derive this relation are based on a recent work by Fendley and Simon [12].

We should note that a related question was discussed previously by Castelnovo and Chamon in Ref. [13], where the authors studied classical variants of a class of quantum double models, including Kitaev's toric code [5]. The authors found that the values of the classical and topological entropy are identical for this class of models. This statement is, in general, no longer true for the classical variants of the string-net states. Instead, we find that

$$\gamma_{\text{classical}} = \ln M, \tag{5}$$

where M is the number of Abelian particles in the anyonic theory underlying the string-net states. Our results shed new light on the significance of the topological entropy in classical systems and gives further insight into what kind of information in the quantum model can be retained in the corresponding classical variant.

Our discussion of the above results is structured as follows in the remainder of the manuscript: We provide a general introduction to the classical Shannon and Renyi entropies in Sec. II. In Sec. III, we introduce the string-net models, first in the context of quantum double models based on the so-called $SU(2)_k$ anyon theories, and then describe their classical analogs. In Sec. IV, we outline the methods we use to analytically compute the Renyi entropies for these classical string-net analogs with the results for the Renyi entropies and the topological entropy of Eq. (5) presented in Sec. V. The manuscript finishes with an outlook on more general string-nets, a summary of our main results, and several appendices providing the details of our calculation.

II. CLASSICAL SHANNON AND RENYI ENTROPY

In quantum mechanics, one of the most important measures of entanglement in a system of multiple quantum mechanical degrees of freedom is the entanglement entropy [14]. We will briefly recap this notion in the following and then turn to the classical analogs of these concepts.

A. Entanglement entropy

Let us consider a quantum system with ground state $|\psi\rangle$ and a bipartition along a smooth cut (without any sharp corners) that divides the system into two parts called A and B. As already outlined in the introduction we can characterize the entanglement of the two partitions by calculating the reduced density matrix of one of the two partitions, say partition A, by tracing out the other one to obtain

$$\hat{\rho}_A = \text{Tr}_B(|\psi\rangle\langle\psi|) .$$

We can now readily diagonalize this reduced density matrix to obtain its eigenvalues p_j, which are the probabilities to find system A in the quantum state corresponding to the respective eigenvector. In terms of these eigenvalues, the entanglement entropy can thus be readily calculated as

$$S_A = -\sum_j p_j \ln p_j . \tag{6}$$

Note that for a quantum system the so-calculated entanglement entropies S_A and S_B are equal, i.e., $S_A = S_B$.

B. Classical entropies

To identify a classical analog to the entanglement entropy, we note that the definition of the entanglement entropy in the form of Eq. (6) has a straightforward interpretation also for classical systems. In particular, we can replace the quantum mechanical probabilities p_j to find the system in a certain state j by their classical counterparts to find subsystem A in a particular classical configuration j_A. The classical analog of the entanglement entropy is then simply given by the well-known Shannon entropy

$$S_A = -\sum_{\{j_A\}} p_{j_A} \ln p_{j_A} , \tag{7}$$

where the sum now runs over the set of all possible configurations $\{j_A\}$ of subsystem A. Similar to the quantum mechanical case, the probability of a given classical configuration j_A is obtained by summing over all possible complementary

configurations in partition B, i.e.,

$$p_{\{j_A\}} = \frac{1}{Z} \sum_{\{j_B\}} e^{-E(\{j_{A+B}\})/(k_B T)} , \tag{8}$$

where $E(\{j_{A+B}\})$ is the energy of the configuration in the full system, k_B is the Boltzmann factor, and T the temperature. Note that, in general, the classical Shannon entropy is not equivalent for the two partitions A and B, i.e., $S_A \neq S_B$.

Instead of directly calculating the Shannon entropy (7) it is often more convenient to compute one of the Renyi entropies

$$S_A^{(n)} = \frac{1}{1-n} \ln \left(\sum_{\{j_A\}} p_{j_A}^n \right) , \tag{9}$$

where the index n typically is an integer $n \geqslant 2$. The Renyi entropies are bounded by each other by $S_{n'} \leqslant S_n$ for $n' > n$, and recover the Shannon entropy in the limit $n \to 1$. They can be computed by considering n copies (replicas) of the system [15]. In doing so, the different replicas of part A are required to have identical configurations, while the configurations in the replicas of part B are independent of one another, see, e.g., Ref. [16] for details of a numerical implementation.

C. Scaling of the entropies and topological corrections

For the ground state of two-dimensional gapped quantum systems, the entanglement entropy obeys an area law, i.e., it grows as the length ℓ of the boundary of system A instead of its volume

$$S_A = c_\ell \ell - \gamma_{\text{quantum}} + \cdots . \tag{10}$$

The coefficient c_ℓ is nonuniversal, as it depends on the microscopic details of the model and can be changed continuously. More interesting is the presence of the subleading constant term γ_{quantum}, which is often called topological entropy and is robust against changing the microscopic details of the system. For a smooth cut, it does neither depend on any length scale of the system nor the geometry of the bipartition and as such must be rooted in long-range entanglement. The seminal work of Refs. [9,10] showed that the topological entropy is universal and can be directly calculated from the total quantum dimension $\mathcal{D}$ of the effective topological field theory. In particular, it is given by $\gamma_{\text{quantum}} = \ln \mathcal{D}$.

As the topological entropy is subleading, it is often cumbersome to determine it to sufficient accuracy by doing a scaling analysis, though recent numerical investigations have been quite successful in doing so [17,18]. In addition, there may be additional $O(1)$ contributions to S_A arising from sharp corners in the cut. Thus, it is beneficial to use a setup, which was introduced by Levin and Wen [10], to extract the topological entropy from a set of different bipartitions of the system as illustrated in Fig. 2. By considering the four different bipartitions of Fig. 2 one can cancel out the leading boundary term in Eq. (10) as well as all $O(1)$ potential corner contributions to directly obtain the topological entropy from the linear combination

$$S_{\text{topo}} = -S_{A_1} + S_{A_2} + S_{A_3} - S_{A_4} , \tag{11}$$

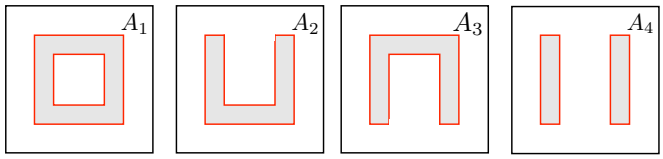

FIG. 2. (Color online) Levin-Wen partitions to compute the topological entropy.

which then leads to the final result

$$S_{\text{topo}} = 2\gamma_{\text{quantum}} . \tag{12}$$

In contrast to the quantum case, the leading term of the classical Shannon entropy S_A scales with the volume V_A of the subsystem A in the bipartition, i.e., it follows a volume law of the general form

$$S_A = c_V V_A + c_\ell \ell - \gamma_{\text{classical}} + \cdots , \tag{13}$$

where ℓ is again the length of the boundary of the partition and the dots indicate subleading terms of order $O(1/\ell)$ that vanish in the limit of $V_A, \ell \to \infty$. Note again that a direct consequence of this volume law is that the Shannon entropy is in general not symmetric with regard to the two partitions, i.e., $S_A \neq S_B$. Similar to the quantum case, we can also in the classical system identify a constant contribution $\gamma_{\text{classical}}$, which reduces the entropy. This constant turns out to be independent of the geometry and size of the system, which is why we will call it "classical topological entropy." As we will discuss in the subsequent sections we can uniquely determine the universal values for this classical topological entropy for a broad variety of classical topologically ordered systems.

At this point, we only want to point out that the form of the scaling behavior of the classical Shannon (and Renyi) entropies still allows to use the setup suggested by Levin and Wen to directly evaluate the $O(1)$ topological correction. One subtle difference to the quantum-mechanical calculation is that in the classical case the topological correction $\gamma_{\text{classical}}$ is sensitive to the number of disconnected regions in partition B. As an example, we show the constant contributions to the entropy for a quantum system and its related classical system for the four Levin-Wen partitions in Fig. 3. The first line indicates the topological entanglement entropy for the quantum mechanical system, the example being the so-called toric code model [5], which has total quantum dimension $\mathcal{D} = 2$. Note that in the quantum-mechanical case, the topological

γ_{quantum}	$2\log 2$	$\log 2$	$\log 2$	$2\log 2$
$\gamma^A_{\text{classical}}$	$\log 2$	0	0	0
$\gamma^B_{\text{classical}}$	0	0	0	$\log 2$

FIG. 3. (Color online) Levin-Wen partitions to compute the topological entropy. Below the partitions is the constant term that is contributed by this bipartitions for the toric code (γ_{quantum}) and the classical loop gas, when computing S_A (γ^A_{cl}) respectively S_B (γ^B_{cl}).

correction for a given bipartition is related to the number of boundaries between parts A and B; the bipartitions involving A_1 and A_4 contribute twice the value than those bipartitions involving A_2 and A_3. The classical analog of the toric code is the so-called loopgas at $T = \infty$, whose classical topological entropy was already studied in Ref. [13] and found to be $\gamma_{\text{classical}} = \ln 2$. As the Shannon entropy is not symmetric in A and B, we show both the topological correction when computing S_A (in the second line) as well as S_B (in the third line). Note that the classical value is independent of the number of boundaries but instead measures the number of disconnected regions in the complementary part. For instance, the topological $O(1)$ contribution in S_A is nonvanishing only if part B is disconnected.

Finally note that the similar setup introduced by Kitaev and Preskill [9] for extracting the topological entropy is not suitable for the classical systems considered here, because all bipartitions have connected parts A and B.

III. CLASSICAL STRING-NET MODELS

As an example family of model systems exhibiting nontrivial topological order, we will consider so-called string-net states and in particular their classical analogs. Their quantum variants, so-called string-net condensed states or simply string-nets, have been introduced by Levin and Wen [19] in a rather general mathematical construction using so-called quantum doubles [20,21]. For completeness, we will briefly recap this Levin-Wen construction in the following by first introducing so-called $SU(2)_k$ anyon theories and then outlining the quantum double construction before shifting gear to discuss the construction of their classical analogs.

A. $SU(2)_k$ anyon theories

The most elementary building block for both the quantum and classical versions of string-nets are so-called $SU(2)_k$ anyon theories [22]. These theories describe anyonic degrees of freedom with both Abelian and non-Abelian exchange statistics (in two spatial dimensions). For a given level k such an anyonic theory contains $k+1$ individual degrees of freedom, which for our purposes here we label by integers

$$0, 1, 2, \ldots k\,.$$

One can think of every degree of freedom as a representation of the quantum group $SU(2)_k$ or in analogy to the spin representation of SU(2), which corresponds to the limit $k \to \infty$, as generalized spins with even/odd integer labels corresponding to integer/half-integer spins.

We can combine two representations of $SU(2)_k$ into one joint representation—similar to combining two spin quantum numbers into one joint spin quantum number for conventional SU(2) spins. This process, which for the anyon theories is often called fusion, has to obey very similar rules as those for combining two conventional SU(2) spins. In particular, they have to obey the so-called fusion rules which also incorporate the cutoff k in a consistent way

$$i \times j = \sum_{l=|i-j|}^{\min[i+j,2k-i-j]} l\,, \tag{14}$$

where l increases in steps of two. Eq. (14) can be written more compactly by introducing fusion coefficients $\mathcal{N}_{ij}^{l}$, which are defined via

$$i \times j \equiv \sum_{l=0}^{k} \mathcal{N}_{ij}^{l}\, l\,. \tag{15}$$

Note that for the $SU(2)_k$ anyon theories at hand these fusion coefficients are always either 0 or 1.

The simplest example is probably the anyon theory $SU(2)_1$ with anyonic degrees of freedom 0 and 1, for which the above fusion rules become

$$0 \times 0 = 0, \quad 0 \times 1 = 1, \quad 1 \times 1 = 0\,. \tag{16}$$

A slightly less trivial example is the anyon theory $SU(2)_2$ with anyonic degrees of freedom 0,1 and 2, for which the fusion rules read

$$1 \times 1 = 0 + 2, \quad 1 \times 2 = 1, \quad 2 \times 2 = 0\,, \tag{17}$$

where the fusion with the identity 0 has been omitted, as it is trivial. In addition we also mention the fusion rules of $SU(2)_3$ with anyonic degrees of freedom 0,1,2, and 3, for which the fusion rules read

$$\begin{aligned} &1 \times 1 = 0 + 2, \quad 1 \times 2 = 1 + 3, \quad 1 \times 3 = 2, \\ &2 \times 2 = 0 + 2, \quad 2 \times 3 = 1, \quad 3 \times 3 = 0, \end{aligned} \tag{18}$$

and, finally, the Fibonacci theory, which is the even-integer subset of this $SU(2)_3$ anyonic theory

$$0 \times 0 = 0, \quad 0 \times 2 = 2, \quad 2 \times 2 = 0 + 2\,. \tag{19}$$

One striking distinction between the fusion rules for $SU(2)_1$ in (16) and for the remaining ones in (17)–(19) is the occurrence of representations, which fused with itself, generate more than one fusion outcome, e.g., representation 1 in $SU(2)_2$. Such representations are called *non-Abelian* as opposed to *Abelian* representations such as the identity 0 that always generate a unique fusion outcome [23]. In order to understand this concept better, let us consider a set comprising multiple such non-Abelian representations. Their combined fusion will no longer be described by a single state but necessarily needs to be described by a set of states. In more technical terms, this manifold of states for a set of non-Abelian degrees of freedom asymptotically grows exponentially with the total number of degrees of freedom. The base of this exponential growth is called the *quantum dimension* d_j of the representation j. Non-Abelian representations have quantum dimensions that are strictly larger than one, i.e., $d_j > 1$. In contrast, any representation i that is Abelian (exhibiting only single fusion outcomes) has quantum dimension $d_i = 1$. For a given anyon theory, the *total quantum dimension* $\mathcal{D}$ is then defined as a sum over all the quantum dimensions of the individual representations of the theory

$$\mathcal{D} = \sqrt{\sum_{j=0}^{k} d_j^2}\,. \tag{20}$$

For all values of k, the $SU(2)_k$ anyon theories always contain two Abelian representations, labeled by 0 and k, with quantum

dimensions $d_0 = d_k = 1$. The remaining representations are all non-Abelian and thus have quantum dimension $d_j > 1$.

B. Quantum double models and string-net condensed states

With the $SU(2)_k$ anyon theories as elementary building blocks at our hand, we can now proceed to briefly recap the quantum double construction of Levin and Wen [19] and introduce the quantum mechanical version of string-net condensed states or simply string-nets.

The quantum double construction of Levin and Wen creates a lattice model from an anyonic theory, such as one of the $SU(2)_k$ anyon theories introduced in the previous section. The elementary constituents of the lattice model are edges that carry an anyonic degree of freedom, which is captured by the respective anyon theory, i.e., it corresponds to one of the labels $0,1,2,\ldots,k$. The bonds form a lattice via *trivalent* vertices. An example of a particularly regular lattice construction would be the honeycomb lattice, which we will use in all visualizations in the following. At each vertex the fusion rules of the anyonic theory need to be fulfilled, thus constraining the possible labelings of edges around a given vertex. Examples of allowed vertices for the $SU(2)_1$, $SU(2)_2$ and Fibonacci theory are given (up to rotations) in the various panels of Fig. 4, respectively.

Forming an entire graph out of a set of these allowed vertices and corresponding edges, one can then create a multitude of lattice configurations. By visual inspection of these configurations it becomes evident how the vertex constraints translate into constraints of the overall lattice configurations. For the case of the $SU(2)_1$ anyonic theory, which contains only Abelian anyons, the resulting configurations will consist of closed loops only, as illustrated in Fig. 5. Introducing a non-Abelian anyon into the anyon theory, as it is the case for, e.g., the Fibonacci theory, the resulting lattice configurations

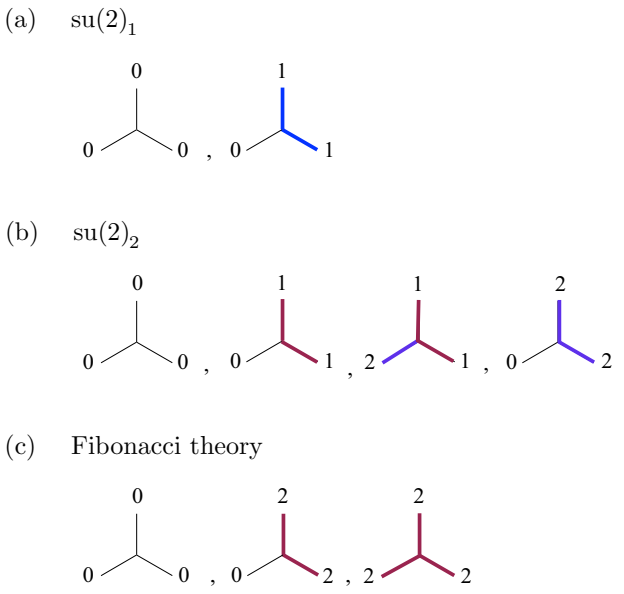

FIG. 4. (Color online) Allowed vertices (up to rotations) for (a) the $SU(2)_1$ anyon theory, (b) the $SU(2)_2$ anyon theory, and (c) the Fibonacci theory.

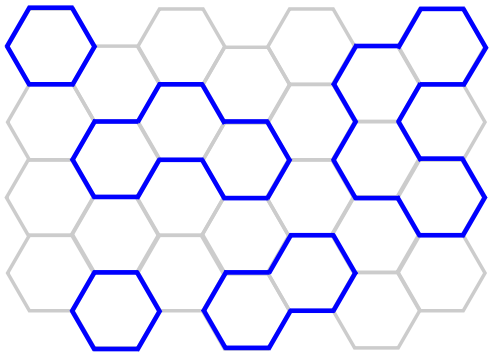

FIG. 5. (Color online) Example of a loop gas configuration for the quantum double model of $SU(2)_1$.

also include branches resulting in netlike configurations as illustrated in Fig. 6.

The set of allowed lattice configurations forms a basis for the part of the Hilbert space, where the ground state resides in. Before moving on to the construction of the classical analog of these quantum states, we want to mention in passing a few additional constraints present in the quantum model (but not the classical model to be introduced in the next section). Most notable for the remainder of this manuscript is that a subset of allowed lattice configurations has vanishing weight for the ground state, in particular, all those configurations where the netlike configuration includes so-called tadpoles illustrated in Fig. 7. The actual weight of an allowed lattice configuration will be finely tuned by a number of parameters depending on the specifics of the underlying anyon theory (such as, e.g., a d-isotopy parameter for the inclusion of closed loops). Further, the Levin-Wen construction goes beyond the construction of quantum ground states, but also allows a description of excited states, e.g., states where the vertex constraint is not fulfilled at individual vertices or which include one of the aforementioned tadpoles.

Finally, we note that in more mathematical terms, the quantum double construction is routed in the so-called Drinfeld double [20], which takes a topological quantum field theory (TQFT) $\mathcal{C}$ and its time-reversal conjugate $\mathcal{C}^*$ to construct a doubled TQFT that is time-reversal invariant [24]. For more

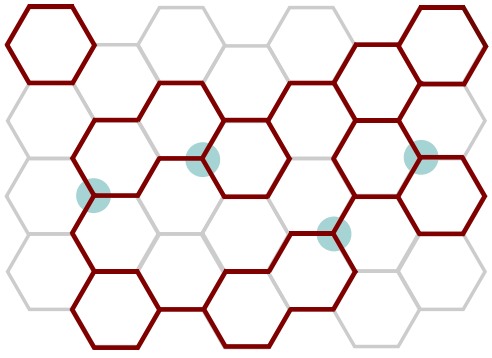

FIG. 6. (Color online) Example of a string-net configuration for the quantum double model of the Fibonacci theory. The circles indicate some of the branching points not present in the loopgas configuration of Fig. 5 for the Abelian $SU(2)_1$ anyon theory.

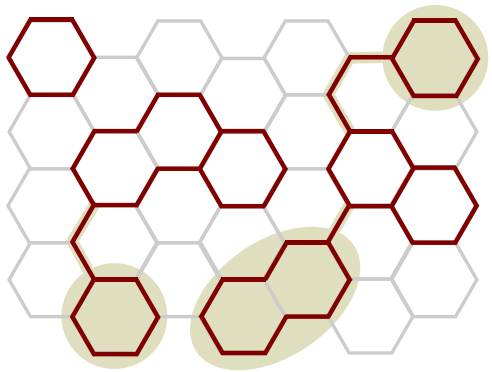

FIG. 7. (Color online) Example of a string-net configuration, which includes so-called tadpoles indicated by the shaded ovals.

details on this construction the reader is referred to the original math literature [20,24] or the more physical introduction in Ref. [21]. Note that the total quantum dimension of the quantum double model is the square of the total quantum dimension of the anyonic theory, i.e., $\mathcal{D}_{\mathrm{QDM}} = \mathcal{D}^2 = \sum_{i=0}^{k} d_i^2$, resulting in a topological entropy $\gamma_{\mathrm{QDM}} = \ln \mathcal{D}^2$.

C. Classical string-nets

We now turn to the classical analogs of the quantum mechanical string-net states introduced as ground states of the quantum double construction of Levin and Wen in the previous section. To do so, we first note that the quantum ground states of Levin and Wen can generally be written as a superposition of string-net configurations s, which fulfill the vertex constraints at every single vertex. The wave function can then be expressed as

$$|\psi\rangle = \sum_s a_s |s\rangle \,, \tag{21}$$

where the coefficients a_s are real, but not necessarily all positive or nonzero [25].

We can now construct a *classical* string-net by defining a partition function that corresponds to the equal-weight superposition of allowed string-net configurations s of the quantum double construction, i.e.,

$$Z[V] = \sum_s 1 \,, \tag{22}$$

where V indicates the number of vertices in the lattice. Note that whether a given string-net configuration s is allowed or not, again depends solely on the *local* constraints implemented around every vertex. In fact, one can explicitly count the number of allowed configurations contributing to the partition function (22). Going through a sequence of combinatorial steps (detailed in Appendix A), one finds that

$$Z[V] = \sum_{j=0}^{k} \left(\frac{\mathcal{D}}{d_j}\right)^V \approx 2\mathcal{D}^V \,, \tag{23}$$

where the d_j indicate the quantum dimension of the anyons in the underlying anyon theory $\mathrm{SU}(2)_k$ and $\mathcal{D}$ is the total quantum dimension of the theory. In the large-volume limit, the explicit sum can be approximated as a power of the total quantum dimension, which connects the original meaning of the quantum dimension in the anyonic theory with its analogous role in the purely classical model.

We should note that one can construct a local Hamiltonian, whose $T = 0$ states are precisely the classical string-nets. To this end, we define the energy E_v of a vertex configuration to be $E_v = 0$, if v fulfills the vertex constraint, and E_v to be a large positive constant otherwise. The energy of a classical configuration is then simply the sum over all the local vertex energies. The partition function of this local Hamiltonian reproduces the expression in Eq. (22) in the $T = 0$ limit.

Before we turn to a general discussion of the classical string-nets defined in this section, we will briefly layout the more technical details of the methods and in particular the role of a so-called crossing symmetry for the analytical calculations of the Renyi entropies for these classical string-nets.

IV. CROSSING SYMMETRY

In the following, we derive several formulas, which are important to the computation of the Shannon or Renyi entropies of the classical string-net models. Our analytical approach is heavily based on the concept of a so-called crossing symmetry, which was recently introduced by Fendley and Simon as a method to compute the exact partition function of a special class of classical lattice model [12]. For later convenience, we will keep the discussion in this section very general, such that it is applicable to *any* crossing symmetric model. As the following discussion of crossing symmetric models is very brief, the interested reader is referred to Ref. [12] for a more complete treatment.

A. Introduction to crossing symmetry

In the following, we consider models that are defined on a trivalent graph with N possible states—labeled by $0,1,2,\ldots N-1$—living on the edges of the graph. The edges are in general oriented, which is indicated by an arrow in the visualizations. We assign each degree of freedom a conjugate via a permutation P of $[0,\ldots,N-1]$ of maximally order two, i.e., $P^2 = 1$. The conjugate of i is denoted by $\bar{i}$ and conjugation is implemented by reversing the arrow on the edge. The physical significance of the conjugation will become clear below.

We define local Boltzmann weights for the vertices that depend on the labels (and orientations) of the three edges around the vertex. When defining the weights $w(i,j,l)$, we use the reference orientation that all arrows are pointing inwards, as is visualized in Fig. 8. The vertex weights can alternatively

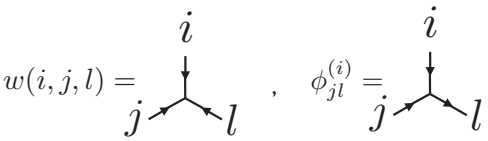

FIG. 8. Definition of the local Boltzmann weight of a vertex configuration.

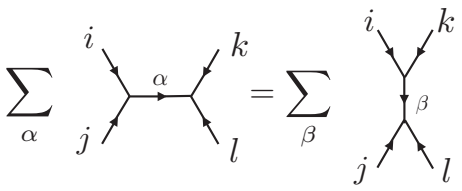

FIG. 9. Graphical representation of crossing symmetry.

be written as a "weight matrix" $\phi^{(i)}$ defined as

$$\phi^{(i)}_{i,j} = w(i,j,\bar{l})\,, \tag{24}$$

which will become convenient later on. Note that the second matrix index is conjugated compared to the definition of the Boltzmann weights, see also Fig. 8. We consider only models that are isotropic, which implies that the value of the Boltzmann weight is the same for cyclic permutations of the indices, i.e., $w(i,j,l) = w(j,l,i) = w(l,i,j)$. The partition function $Z[V]$ of a graph with V vertices is then defined as the sum over all edge labelings of the product of all weights

$$Z[V] = \sum_{\text{edgelabels}} \prod_{\text{vertices}\nu} w(i_\nu, j_\nu, l_\nu)\,. \tag{25}$$

The model is called crossing symmetric if the Boltzmann weights defined on the vertices fulfill the crossing symmetry relation

$$\sum_{\alpha=0}^{N-1} w(i,j,\bar{\alpha})w(\alpha,l,k) = \sum_{\beta=0}^{N-1} w(k,i,\bar{\beta})w(\beta,j,l)\,, \tag{26}$$

which is visualized in Fig. 9.

Crossing symmetry implies that the weight matrices (24) commute. In Ref. [12], Fendley and Simon showed that crossing symmetry allows for calculating the partition function exactly. Using the crossing symmetry relation (26) successively, one can equate the partition function of different graphs. This in turn allows a transformation to a graph, where the partition function can be calculated straightforwardly. An example of such a transformation is illustrated in Fig. 10. The main insight is that the graph can always be deformed into a chain of "bubbles," where a bubble can be interpreted as a matrix that in the following is denoted by T and defined through the weight matrices (24)

$$T = \sum_{s=0}^{N-1} \phi^{(s)}\phi^{(\bar{s})}\,. \tag{27}$$

By definition, the T matrix commutes with all the weight matrices. The graphical interpretation of the bubble as a matrix

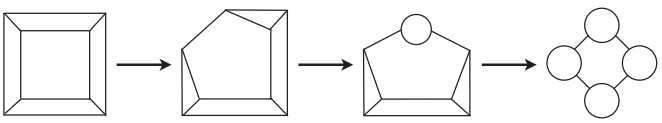

FIG. 10. Using crossing symmetry equates the partition function of different graphs. Any planar, closed graph can be reduced to a chain of bubbles (rightmost graph).

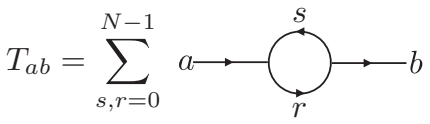

FIG. 11. Graphical representation of the matrix elements T_{ab}.

is visualized in Fig. 11. As a result of the transformation of the graph, the evaluation of the partition function is reduced to diagonalizing an $N \times N$ matrix

$$Z[V] = \mathrm{Tr}(T^{V/2})\,. \tag{28}$$

B. Examples of crossing symmetric models

The crossing symmetry relation (26) seems at first glance rather restrictive. However, there are a number of interesting classical models that obey the relation. In particular, it was shown in Ref. [12] that the classical string-net models discussed in Sec. III C are crossing symmetric. To be more precise, the degrees of freedom living on the edges are the representations of the $\mathrm{SU}(2)_k$ anyon theory. Admissible string-net configurations have the property that the fusion rules are fulfilled at each vertex. This constraint corresponds to a local Boltzmann weight of

$$w(i,j,l) = \mathcal{N}_{ij}^{\bar{l}}\,, \tag{29}$$

where the ordering of the labels is not important, i.e.,

$$w(i,j,l) = w(j,i,l)\,.$$

The conjugate $\bar{i}$ of the degree of freedom i is defined as the unique element, such that the fusion of i and its conjugate contains the identity element 0, i.e., $i \times \bar{i} = 0 + \cdots$. From the fusion rules of the $\mathrm{SU}(2)_k$ anyon theory, it can readily be seen that the identity element only occurs when $\bar{i} = i$. Hence all degrees of freedom are their own conjugate in this case and we can consider the edges as unoriented. However, this is no longer true for more complicated anyon theories, such as e.g., $\mathrm{SU}(N)_k$.

Another class of crossing symmetric models are the ones based on finite groups. The degrees of freedom living on the edges are now taken to be elements of a finite group G with the identity element denoted by e. In this manuscript, we are most interested in models, where the group operation $\circ$ is fulfilled at each vertex, i.e.,

$$w(i,j,l) = \begin{cases} 1 & \text{if} \quad i \circ j \circ l = e, \\ 0 & \text{otherwise}\,. \end{cases} \tag{30}$$

The conjugate element $\bar{i}$ of i is defined as the unique inverse, such that $i \circ \bar{i} = \bar{i} \circ i = e$. When G is non-Abelian the ordering of the indices in $w(i,j,l)$ is important, i.e., in general, $w(i,j,l) \neq w(i,l,j)$. As a result, we need to introduce an orientation for each vertex (in addition to the orientation of the edges). Here, we use the convention that the ordering of the indices corresponds to an anticlockwise orientation of the vertex.

We should comment on that Eq. (30) is, in fact, much more restrictive than is needed for crossing symmetry, as was shown

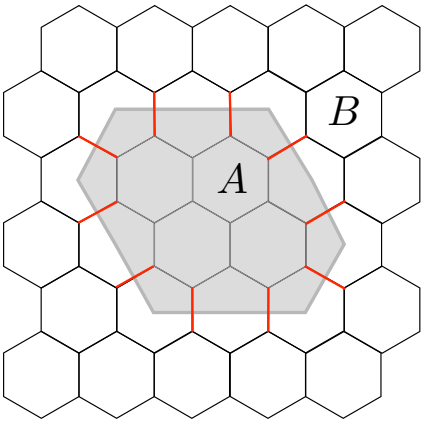

FIG. 12. (Color online) Bipartition of the lattice into two regions A (in grey) and B. The system is cut on the edges, with the ℓ boundary edges marked in red.

in Ref. [12]. However, the models defined by (30) are the most interesting from the perspective of calculating the Renyi entropies, as it turns out that they have the maximal possible value of the topological entropy, namely $\ln|G|$, where $|G|$ is the number of elements in G.

C. Renyi entropy of crossing symmetric models

Having already derived an explicit expression for the partition function in Eq. (28), let us now continue with discussing the relevant steps to compute the Renyi entropies. When dividing the system into two partitions A and B, we divide the set of vertices spatially into vertices in A and B, respectively, thus cutting the graph spatially on the edges. The total number of these 'boundary edges' is denoted by ℓ in the following. As the two subsystems A and B are only coupled via the boundary links, it is useful to keep the boundary configuration, denoted by $\boldsymbol{\alpha} = (\alpha_1, \ldots, \alpha_\ell)$, explicit. A visualization of a bipartition of the system with boundary configuration $\boldsymbol{\alpha}$ can be found in Fig. 12.

In order to compute the Renyi entropies, we need an expression for the probability $p_{\{I,\boldsymbol{\alpha}\}}$ of a given configuration $\{I,\boldsymbol{\alpha}\}$, where the set I incorporates all edge labels in the volume (excluding the boundary) of one of the partitions, say A. In terms of the local Boltzmann weights $w(i,j,l)$, the probability is given by

$$p_{\{I,\boldsymbol{\alpha}\}} = \frac{1}{Z}\prod_{v\in A} w(i_v,j_v,l_v)\sum_B\prod_{v\in B} w(i_v,j_v,l_v)\,, \tag{31}$$

where $\sum_B$ indicates a sum over all edge labels of links in B (again excluding the boundary). Inserting the probability into the definition of the Renyi entropy with index n yields

$$S_n^A = \frac{1}{1-n}\ln\left[\sum_{\boldsymbol{\alpha}}\left(\sum_A\prod_{v\in A} w(i_v,j_v,l_v)^n\right)\times\left(\frac{\sum_B\prod_{v\in B} w(i_v,j_v,l_v)}{Z}\right)^n\right]. \tag{32}$$

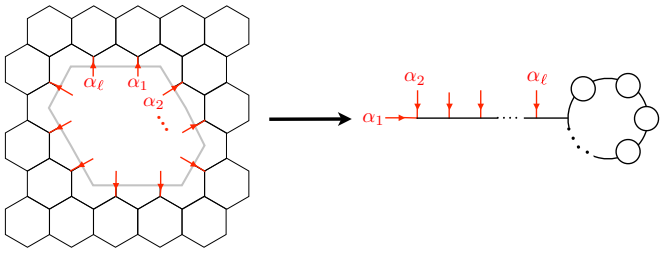

FIG. 13. (Color online) Graphical representation of how to use crossing symmetry to compute $W_1(\boldsymbol{\alpha},V)$, Eq. (34). The boundary is indicated in grey and the boundary edges as well as their orientation are marked in red.

In order to simplify this expression, we define a "boundary weight" $W_n(\boldsymbol{\alpha},V_B)$ (and similarly for A) by

$$W_n(\boldsymbol{\alpha},V_B) = \sum_B\prod_{v\in B} w(i_v,j_v,l_v)^n\,, \tag{33}$$

where V_B denotes the volume of B and is defined such that $V_B+\ell$ is the total number of vertices in B. This definition ensures that the contributions of the volume and the boundary to the Renyi entropy are nicely separated in the final result.

$W_1(\boldsymbol{\alpha},V_B)$ is nothing but the total weight of classical configurations in B, given a particular boundary configuration $\boldsymbol{\alpha}$. It can be computed exactly by using crossing symmetry to transform the graph of subsystem B into one, where the internal summation over all edge labelings in B is expressed as a matrix power of the T matrix (27):

$$W_1(\boldsymbol{\alpha},V_B) = \sum_{\beta=0}^{M-1}[\phi^{(\alpha_2)}\ldots\phi^{(\alpha_\ell)}]_{\alpha_1,\beta}\mathrm{Tr}(\phi^{(\beta)}T^{V_B/2})\,. \tag{34}$$

An example of such a transformation is illustrated in Fig. 13. As the weight matrices $\phi^{(\alpha)}$ commute with each other as well as with the T matrix, we can simultaneously diagonalize them and Eq. (34) can be readily expressed in terms of the eigenvalues of the matrices. Note that we must define a reference configuration on the boundary edges, in the case where edges have an orientation. In the following, we will use the convention that the arrows point towards the vertices in the respective volume, i.e., B in case at hand. Consequently, we need to take the conjugate boundary configuration $\bar{\boldsymbol{\alpha}} = (\bar{\alpha}_1,\ldots,\bar{\alpha}_\ell)$ for the boundary weight of the other partition, which is A in this case.

If the replicated system is crossing symmetric, i.e., if the weights $w(i,j,l)^n$ obey the crossing symmetry relation (26), we can also compute $W_n(\bar{\boldsymbol{\alpha}},V_A)$ exactly, using the weight matrices and the T matrix that are obtained from the weights $w(i,j,l)^n$ instead. As a result, we can find a compact expression for the Renyi entropy of subsystem A with index n:

$$S_n^A = \frac{1}{1-n}\ln\left[\sum_{\boldsymbol{\alpha}} W_n(\bar{\boldsymbol{\alpha}},V_A)\left(\frac{W_1(\boldsymbol{\alpha},V_B)}{Z}\right)^n\right], \tag{35}$$

for all classical models, where the model as well as the replicated model—i.e., the model, where the local Boltzmann weights are given by $w(i,j,l)^n$—are crossing symmetric.

The requirement that both $w(i,j,l)$ as well as $w(i,j,l)^n$ obey the crossing symmetry relation seems at first glance rather restrictive. However, we note that for the classical string-net models based on the $SU(2)_k$ anyon theories the weights $w(i,j,l)$ are all either 0 or 1. Hence, the replicated model is trivially crossing symmetric. The same applies to a few other string-net models, e.g., those based on the $SU(N)_k$ theories with $k = 1,2$. It is also valid for the classical models based on finite groups that were discussed in the previous section.

V. RENYI ENTROPY OF CLASSICAL STRING-NET MODELS

In this section, we give a brief outline on how to derive the Shannon and Renyi entropies of classical string-net models and discuss their properties. We focus on the model based on the $SU(2)_k$ anyon theory, for which we provide the basic steps. A detailed derivation can be found in Appendix A.

Let us first discuss a bipartition, where part A and B are both connected, for instance A_2 and A_3 in Fig. 3. We note that for the classical string-net based on the $SU(2)_k$ anyon theory, all representations are self-conjugate and the local Boltzmann weight of a vertex is either 0 or 1. Consequently, the expression for the Renyi entropy (35) simplifies to the following:

$$S_n^A = \frac{1}{1-n} \ln \left[\sum_{\boldsymbol{\alpha}} W_1(\boldsymbol{\alpha}, V_A) \left(\frac{W_1(\boldsymbol{\alpha}, V_B)}{Z} \right)^n \right]. \quad (36)$$

The partition function $Z[V]$, see Eq. (23), can be approximated by

$$Z[V] \approx 2\mathcal{D}^V \quad (37)$$

in the limit of large volume V. In the following, we assume that both the volume of partition A and B are large, such that the approximation above is valid. The boundary weights $W_1(\boldsymbol{\alpha}, V)$ can then be expressed in terms of the quantum dimensions of the representations in the $SU(2)_k$ anyon theory

$$W_1(\boldsymbol{\alpha}, V) = \begin{cases} 2\mathcal{D}^V \prod_{j=0}^k d_j^{n_j} & \text{if } \left(\sum_{s=1}^{\ell} \alpha_s\right)/2 \in \mathbb{N} \\ 0 & \text{otherwise} \end{cases}, \quad (38)$$

where n_j is the number representations of type j in the boundary configuration. Deriving Eq. (38) makes use of the fact that the eigenvalues of the weight matrices are related to the quantum dimensions, which we derive in Appendix A. Crossing symmetry implies that the ordering in the boundary configuration is irrelevant, only the number of each type of representation enters the expression for the weight. The summation over all boundary configurations can be performed by noting that the summands are nothing but multinomial coefficients of $(\mathcal{D}_{n+1}^{\pm})^{\ell}$ with

$$\mathcal{D}_m^{\pm} = \sum_{j=0}^{k} (\pm 1)^j d_j^m, \quad (39)$$

and the Renyi entropy becomes

$$\begin{aligned} S_n^A &= V_A \ln \mathcal{D} + \frac{2n\ell}{n-1} \ln \mathcal{D} + \frac{1}{1-n} \ln \left({\mathcal{D}_{n+1}^+}^{\ell} + {\mathcal{D}_{n+1}^-}^{\ell} \right) \\ &\approx V_A \ln \mathcal{D} + \ell \ln \left(\frac{\mathcal{D}^{2n}}{\mathcal{D}_{n+1}^+} \right)^{1/(n-1)}, \end{aligned} \quad (40)$$

where the second line is valid in the limit of a long boundary length ℓ.

Note that there is no constant contribution to the Renyi entropy, when part A and B are both connected. The constraint of the boundary—there are only $\frac{1}{2}k^{\ell}$ instead of k^{ℓ} boundary configurations that contribute to the entropy—is exactly compensated by the constraint from the volume, i.e., the factor 2 in the boundary weights $W_1(\boldsymbol{\alpha}, V)$ in Eq. (38) as well as the partition function (28) in Eq. (37). Note that this additional factor came about because there are two Abelian representations in the $SU(2)_k$ model, which resulted in that the highest eigenvalue of T matrix (27) was doubly degenerate.

Let us now assume that part A is connected, but there are two disconnected regions in B denoted by B_1 and B_2, e.g., bipartition A_1 in Fig. 3. The boundary configuration for $B_1(B_2)$ is given by $\boldsymbol{\alpha}_1(\boldsymbol{\alpha}_2)$ with length $\ell_1(\ell_2)$. The expression for the weights $W_1(\boldsymbol{\alpha}, V)$ in Eq. (38) is unchanged, except that the weight for part A has a boundary that is the combination of $\boldsymbol{\alpha}_1$ and $\boldsymbol{\alpha}_2$. That the boundaries combine and can be written as one boundary of length $\ell = \ell_1 + \ell_2$ is ensured by crossing symmetry. The calculation of the Renyi entropy proceeds along the same lines as the one above, but in this case the boundary and volume constraints do not compensate each other. Instead, the constraints arising from the volume are only partly compensated by the boundary, which yields an additional $-\ln 2$ to the previous result:

$$\begin{aligned} S_n^A &= V_A \ln \mathcal{D} + \frac{2n\ell}{n-1} \ln \mathcal{D} \\ &\quad + \frac{1}{1-n} \ln \left(\sum_{\sigma_1, \sigma_2 = \pm 1} \mathcal{D}_{n+1}^{\sigma_1 \ell_1} \mathcal{D}_{n+1}^{\sigma_2 \ell_2} \right) - \ln 2 \\ &\approx V_A \ln \mathcal{D} + \ell \ln \left(\frac{\mathcal{D}^{2n}}{\mathcal{D}_{n+1}^+} \right)^{1/(n-1)} - \ln 2, \end{aligned} \quad (41)$$

where the second line is valid when ℓ_1 and ℓ_2 are both large. If we had computed S_n^B instead, we had recovered expression (40) with A and B interchanged.

The calculation above is straightforward to generalize to arbitrary number of regions in A and B. We find that in the limit, where the individual volumes and boundary lengths are all large, the Renyi entropy is given by

$$S_n^A = V_A \ln \mathcal{D} + \ell \ln \left(\frac{\mathcal{D}^{2n}}{\mathcal{D}_{n+1}^+} \right)^{1/(n-1)} - (n_b - 1) \ln 2, \quad (42)$$

where n_b is the number of disconnected regions in part B. Analytic continuation to $n = 1$, gives the following result for the Shannon entropy:

$$S_A = V_A \ln \mathcal{D} + \ell \ln \left[\mathcal{D}^2 \prod_{j=0}^{k} (d_j)^{-d_j^2/\mathcal{D}^2} \right] - (n_b - 1) \ln 2. \quad (43)$$

Let us emphasize again that the total quantum dimension $\mathcal{D}$ of the anyon theory appears as coefficient in the volume term, but not in the topological entropy. The latter is instead given by the logarithm of the number of Abelian representations, which is two for *all* $SU(2)_k$ anyon theories. In Appendix C, we present an alternative description of the $SU(2)_k$ models, which gives

an intuitive understanding of this, at first glance surprising, finding that the topological entropy does not depend the level k. It turns out that all classical string-net models based on the $SU(2)_k$ anyon theories can be mapped to generalized loop models, for which an topological entropy of $\ln 2$ is expected, independent on the details of the loop model.

VI. OUTLOOK

So far, we have focused our discussion on classical string-nets rooted in the $SU(2)_k$ anyon theories. However, the quantum double construction of Levin and Wen and as such also the construction of their classical analogs can in principle be applied to a much broader class of anyonic theories (or in more general words topological quantum field theories). For the $SU(2)_k$ anyon theories, we have found that the topological entropy is $\gamma_{\text{classical}} = \ln 2$, independent of the level k of the theory. In fact, this result can readily be generalized to a broader class of anyon theories to

$$\gamma_{\text{classical}} = \ln M,$$

where M is the number of Abelian representations in the underlying anyon theory. It might thus be interesting to go to anyonic theories that contain more than the strictly two Abelian representations in the $SU(2)_k$ theories. One prominent example is the family of $SU(N)_k$ anyon theories, which we will touch on in the next section. Another example would be models based on finite groups G, which we will briefly discuss in the subsequent section.

A. $SU(N)_k$ models

We first consider string-net models based on the $SU(N)_k$ anyon theories, which are related the more conventional SU(N) algebra, in that only a finite number of representations is kept—similar to the $SU(2)_k$ deformation of SU(2) discussed before. The theory contains $\binom{k+N-1}{N-1}$ representations, N of which are Abelian. The fusion rules can again be constructed—similar to the fusion rules (14) of $SU(2)_k$—in a consistent way that incorporates the cutoff k of the deformation, though no closed expression are known for $N > 3$.

Constructing the classical string-net model based on these $SU(N)_k$ anyon theories we can again define a set of admissible lattice configurations, where the fusion rules are fulfilled at every single vertex. A (weighted) sum over these admissible lattice configurations will then define the partition function of the classical model. Similar to our discussion of the $SU(2)_k$ string-net models we define the local Boltzmann weight of a vertex via the fusion rules as

$$w(i,j,l) = \mathcal{N}_{ij}^{\bar{l}},$$

which not only enforces the fusion rules at the vertex, but also assigns weights to the various admissible vertex configurations. In particular, it should be noted that for $k > 2$ not all vertices enter with the same weight, but depending on the multiplicity of certain fusion channels $\mathcal{N}_{ij}^{l}$ the weights can actually vary—in contrast to the previously discussed case of $SU(2)_k$ anyon theories.

The so-defined classical $SU(N)_k$ string-net model obeys the crossing symmetry relation (26) [12]. However, as a consequence of the unequal Boltzmann weights for $k > 2$ the replicated system used for calculation of the Renyi entropies no longer obeys the crossing symmetry. As such, our results can be directly generalized only to the case of $su(N)_1$ and $SU(N)_2$ anyon theories, while the $SU(N)_k$ theories with $k > 2$ require additional work beyond the scope of the current manuscript.

Let us first get some intuition by discussing the $su(N)_1$ anyon theory, which turns out to be rather accessible. It has N representations, which can be labeled consecutively by integers $0, \ldots, N-1$. All representation are Abelian with fusion rules

$$i \times j = (i + j) \mod N, \tag{44}$$

where we note that these fusion rules are equivalent to the group operation of the cyclic group $\mathbb{Z}_N$.

The fusion matrices are then given by

$$\phi_{ij}^{(\alpha)} = \delta_{(\alpha+i) \bmod N, j} \tag{45}$$

and the T matrix is diagonal with

$$T = N\,\mathbf{1}_N. \tag{46}$$

From the definition of the weight (34), one can deduce that only configurations, where the boundary representations fuse to the identity, contribute to the Renyi entropies

$$W_1(\boldsymbol{\alpha}, V) = \begin{cases} N^{V/2+1} & \text{if} \quad \left(\sum_{j=1}^{\ell} \alpha_j\right) \bmod N = 0, \\ 0 & \text{otherwise}. \end{cases} \tag{47}$$

Inserting the weights into (35) and noting that there are $N^{\ell-1}$ allowed boundary configurations for each individual boundary, one obtains the Renyi entropy

$$S_n^A = V_A \ln \sqrt{N} + \ell \ln N - (n_b - 1) \ln N, \tag{48}$$

where n_b is the number of disconnected regions in B. We again see that the Renyi entropy follows a volume law augmented by a boundary term and a topological correction of the form

$$\gamma_{SU(N)_1} = \ln N. \tag{49}$$

This result is precisely in line with the statement that only the number of Abelian anyons in the underlying anyonic theory contributes to the topological correction.

The calculation for $SU(N)_2$ is substantially more technical, but yields precisely the same value for the topological entropy

$$\gamma_{SU(N)_2} = \ln N. \tag{50}$$

The interested reader is referred to Appendix B for some of the details of this calculation.

B. Finite groups

In addition to anyon models described so far, the quantum double construction, the formulation of its classical analog as well as the methods described to calculate the classical entropies in section V can also be used to study classical string-net models based on finite groups, both Abelian and non-Abelian. Such a group is denoted by G in the following and its elements by $e, i, j, \ldots \in G$ with e being the identity element. The fusion rules are replaced by the usual group operation $\circ$, such that

$$i \circ j = l$$

implies a "fusion coefficient"

$$\mathcal{N}_{ij}^{l} = \delta_{i\circ j\circ \bar{l},e}\,,$$

where $\bar{i}$ is the (unique) inverse of i defined by $i\circ\bar{i} = \bar{i}\circ i = e$. The Boltzmann weights are thus defined as

$$w(i,j,l) = \begin{cases} 1 & \text{if} \quad i\circ j\circ l = e, \\ 0 & \text{otherwise}\,. \end{cases} \tag{51}$$

We want to emphasize, the outcome of "fusing" two particles is always unique given an ordering. Thus all elements are Abelian according to our previous definition counting the number of fusion outcomes, even though the underlying group may be non-Abelian. In particular, the individual quantum dimensions are all $d_j = 1$ and the total quantum dimension $\mathcal{D} = \sqrt{|G|}$, where $|G|$ is the total number of elements in the group. The calculation of the Renyi entropy is very similar to the one outlined for $\mathrm{su}(N)_1$. In particular, Eq. (48) still holds when replacing N by $|G|$:

$$S_n^A = V_A \ln\sqrt{|G|} + \ell \ln|G| - (n_b - 1)\ln|G|\,. \tag{52}$$

Finally, we should emphasize that our results for classical models based on finite groups are fully consistent with the results previously reported by Castelnovo and Chamon in Ref. [13]. See also Ref. [26] for related work on Kagome spin ice.

VII. SUMMARY

To summarize our results, the manuscript at hand provides a detailed introduction of the construction of classical string-net models from quantum double models based on a given anyon theory. For the family of $\mathrm{SU}(2)_k$ anyon theories, we have carefully analyzed the topological entropies arising as subleading contribution in the Renyi entropies. In particular, we have derived the precise form of the volume law governing the Renyi entropies of order n for a subsystem A

$$S_n^A = V_A \ln\mathcal{D} + \ell \ln\left[\frac{\mathcal{D}^{2n}}{\mathcal{D}_{n+1}^{+}}\right]^{\frac{1}{(n-1)}} - (n_b - 1)\ln 2\,, \tag{53}$$

where n_b is the number of disconnected regions in part B, $\mathcal{D}$ is the total quantum dimension (20) of the anyon theory and $\mathcal{D}_m^{+} = \sum_{j=0}^{k} d_j^m$.

Analytic continuation to $n = 1$ yields the Shannon entropy

$$S_A = V_A \ln\mathcal{D} + \ell \ln\left[\mathcal{D}^2 \prod_{j=0}^{k} (d_j)^{-d_j^2/\mathcal{D}^2}\right] - (n_b - 1)\ln 2\,. \tag{54}$$

These results for the $\mathrm{SU}(2)_k$ anyon theories can readily be generalized to $\mathrm{SU}(N)_k$ theories with $k = 1,2$ as well as models based on finite groups to give a topological entropy of

$$\gamma = \ln M, \tag{55}$$

where M is the number of Abelian representations in the underlying anyon theory. Eq. (55) is the main result of our manuscript.

Let us finally reemphasize that the classical and quantum variants of topological entropy are encoding substantially different aspects of the system, even though they are defined in a very similar manner. While the quantum topological entropy arises from a constraint on the boundary, the classical entropy rather originates from a constraint on the volume. In particular, in the quantum system, the topological $O(1)$ contribution is proportional to the number of individual boundaries. For the classical counterpart, the Shannon (or Renyi) entropy of subsystem A has a topological contribution, which is proportional to the number of disconnected regions in subsystem B, or rather $n_b - 1$. Even though the actual values of the classical and quantum topological entropy can turn out to be the same, in particular when considering classical models based on finite groups [13], they are, in general, sensitive to different features in the topological field theory. While the quantum version is sensitive to all representations in the quantum double model of the underlying anyon theory, the classical one is sensitive only to the Abelian ones in the anyon theory—resulting in vastly different estimates for $\mathrm{SU}(2)_k$ anyon theories with $k \geqslant 2$.

Unfortunately, the proof leading to (55) does not directly generalize to $\mathrm{SU}(N)_k$ for arbitrary k, as the summation over configurations in part A and the boundary cannot be performed analytically. The form of Eq. (35) suggests that the topological contribution is again given by $(n_b - 1)\ln N$. However, within our current approach we cannot rigorously proof that there are no other contributions to the topological entropy arising, e.g., from the summation over boundary configurations. For these cases, numerical simulations might be useful to shed more light on this question.

An important issue that was not discussed in this manuscript is the one of stability. The main feature of the topological entropy of quantum systems is that it is robust against any kind of local perturbations. It was already noted in Ref. [13] that the classical topological entropy is not robust against softening the vertex constraint. Let us for instance consider the classical loop model. As soon as there is a finite (even if infinitesimal) probability of open loops, the topological entropy vanishes for large enough system sizes. Another important perturbation in the classical string-net model is introducing a string tension. Some guidance on this issue arises from the classical loop model. The latter is dual to the 2D Ising model with the loop tension in the loop model corresponding to finite temperature in the Ising model. As such we know that the (topologically nontrivial) loop gas phase persists up to a finite, critical loop tension, corresponding precisely to the critical temperature of the dual Ising model. As such it is reasonable to expect that the topological entropy remains constant up to the critical value of the loop tension. The topological entropy of the classical system can then be used to characterize an entire phase in full analogy to its quantum counterpart.

ACKNOWLEDGMENTS

M.H. thanks Eddy Ardonne, Steve Simon, and Joost Slingerland for interesting and stimulating discussions. S.T. thanks R. G. Melko for an inspiring discussion that has led to the idea for the calculations in the manuscript at hand. We also thank T. Quella for a critical reading of the manuscript. We acknowledge partial support from SFB TR 12 of the DFG.

APPENDIX A: RENYI ENTROPY FOR THE SU(2)$_K$ STRING-NET

In this Appendix, we derive the analytic expression of the Renyi entropies for SU(2)$_k$ string-nets in the limit of large volume. We focus on a bipartition, where part A and B are both connected. Generalizing to disconnected regions in B and/or A is straightforward.

The weight matrices and the T matrix are simultaneously diagonalized by the modular S matrix, which is known explicitly for SU(2)$_k$, see, e.g., Ref. [27]:

$$S_{ij} = \sqrt{\frac{2}{k+2}} \sin\left[\frac{(i+1)(j+1)}{k+2}\pi\right] \tag{A1}$$

with $i,j = 0,\ldots,k$. The explicit form of the S matrix is in fact not important for the proof. However, we will use that the S-matrix elements are directly related to the quantum dimensions d_j of the representations of the SU(2)$_k$ anyon theory:

$$S_{00} = \mathcal{D}^{-1}, \quad S_{j0} = S_{0j} = \frac{d_j}{\mathcal{D}}, \tag{A2}$$

where $\mathcal{D}$ is the total quantum dimension (20). Consequently, the eigenvalues of the weight matrices and the T matrix

$$[S^\dagger \phi^{(\alpha)} S]_{i,j} = \delta_{i,j}\lambda_j^{(\alpha)}, \quad [S^\dagger T S]_{i,j} = \delta_{i,j} t_j \tag{A3}$$

are also related to the quantum dimensions:

$$\lambda_j^{(\alpha)} = \frac{S_{\alpha j}}{S_{0j}}, \quad t_j = \left(\frac{\mathcal{D}}{d_j}\right)^2. \tag{A4}$$

In particular,

$$\lambda_0^{(\alpha)} = d_\alpha, \quad \lambda_k^{(\alpha)} = (-1)^\alpha d_\alpha, \tag{A5}$$

which can readily be derived from (A1). For SU(2)$_k$ there are exactly two Abelian representations, labeled by 0 and k, with $d_0 = d_k = 1$. All other represenations are non-Abelian and have, therefore, larger quantum dimensions. Thus the highest eigenvalue of the T-matrix has value $\mathcal{D}^2$ and is twofold degenerate. As a consequence, we find that the partition function (28) grows asymptotically as a power of the total quantum dimension $\mathcal{D}$,

$$Z[V] = \sum_{j=0}^{k}\left(\frac{\mathcal{D}}{d_j}\right)^V \approx 2\mathcal{D}^V, \tag{A6}$$

in the limit of large V.

Let us now proceed by deriving an explicit formula for the boundary weight (34). In the following, we assume that the volumes of both subsystems are large. The boundary weight of a boundary configuration $\boldsymbol{\alpha}$ and volume V is by definition

$$\begin{aligned} W_1(\boldsymbol{\alpha},V) &= \sum_{\beta=0}^{k}[\phi^{(\alpha_1)}\ldots\phi^{(\alpha_\ell)}]_{0,\beta}\mathrm{Tr}[\phi^{(\beta)}T^{V/2}] \\ &= \sum_{\beta,s,j=0}^{k} S_{0j}\lambda_j^{(\alpha_1)}\ldots\lambda_j^{(\alpha_\ell)}S_{\beta j}\lambda_s^{(\beta)}\left(\frac{\mathcal{D}}{d_s}\right)^V. \end{aligned} \tag{A7}$$

Using the explicit expression of $\lambda_s^{(\beta)}$ in terms of the S-matrix elements, performing the summation over β and noting that $SS^\dagger = S^\dagger S = \mathbf{1}_{k+1}$ yields

$$W_1(\boldsymbol{\alpha},V) = \sum_{s,j=0}^{k}\delta_{j,s}\lambda_j^{(\alpha_1)}\ldots\lambda_j^{(\alpha_\ell)}\left(\frac{\mathcal{D}}{d_s}\right)^V. \tag{A8}$$

In the large-volume limit, only the terms with $s = 0,k$ survive, the others are exponentially suppressed. By noting that Eq. (A5) relates the 0th and kth eigenvalue of the weight matrices to the quantum dimension, we arrive at the final result for the boundary weight

$$\begin{aligned} W_1(\boldsymbol{\alpha},V) &= [1+(-1)^\Sigma]\mathcal{D}^V\prod_{j=1}^{\ell}\lambda_0^{(\alpha_j)} \\ &= [1+(-1)^\Sigma]\mathcal{D}^V\prod_{j=0}^{k}{d_j}^{n_j}, \end{aligned} \tag{A9}$$

where $\Sigma = \sum_{j=0}^{\ell}\alpha_j$ and n_j is the multiplicity of the representation labeled by j on the boundary. The ordering of the representations is unimportant due to crossing symmetry.

Using the explicit form of the boundary weights, the Renyi entropy can be computed straightforwardly:

$$\begin{aligned} S_n^A &= \frac{1}{1-n}\ln\left[\sum_{\boldsymbol{\alpha}}W_1(\boldsymbol{\alpha},V_A)\left(\frac{W_1(\boldsymbol{\alpha},V_B)}{Z}\right)^n\right] \\ &= \frac{1}{1-n}\ln\left\{\sum_{n_0+\ldots+n_k=\ell}\frac{\ell!}{n_0!\ldots n_k!}\right. \\ &\quad\left.\times\prod_{j=0}^{k}(d_j)^{n_j(n+1)}[1+(-1)^\Sigma]^{n+1}\right\} \\ &\quad+\frac{1}{1-n}\ln[\mathcal{D}^{V_A+nV_B-n(V_A+V_B+2\ell)}2^{-n}], \end{aligned} \tag{A10}$$

where the binomial factors enumerate the number of configurations for given $n_0,\ldots,n_k$. Using $[1+(-1)^\Sigma]^{n+1} = 2^n[1+(-1)^\Sigma]$ and $\Sigma = \sum_{j=0}^{k} jn_j$, we find that

$$\begin{aligned} S_n^A &= V_A\ln\mathcal{D} + \frac{2n\ell}{n-1}\ln\mathcal{D} \\ &\quad+\frac{1}{1-n}\ln\left\{\sum_{n_0+\ldots+n_k=\ell}\frac{\ell!}{n_0!\ldots n_k!}\prod_{j=0}^{k}\left(d_j^{(n+1)}\right)^{n_j}\right. \\ &\quad\left.+\sum_{n_0+\ldots+n_k=\ell}\frac{\ell!}{n_0!\ldots n_k!}\prod_{j=0}^{k}\left[(-1)^j d_j^{(n+1)}\right]^{n_j}\right\}, \end{aligned} \tag{A11}$$

where the last two lines are multinomial expansions of $(\mathcal{D}_{n+1}^{\pm})^\ell$ with

$$\mathcal{D}_m^{\pm} = \sum_{j=0}^{k}(\pm 1)^j(d_j)^m. \tag{A12}$$

We can simplify Eq. (A11) by noting that the contribution from $\mathcal{D}_{n+1}^{-}$ vanishes exponentially in the limit of large ℓ and obtain

$$S_n^A = V_A \ln \mathcal{D} + \ell \ln \left(\frac{\mathcal{D}^{2n}}{\mathcal{D}_{n+1}^{+}} \right)^{1/(n-1)} . \quad \text{(A13)}$$

In the limit $n \to 1$, we find the following limiting behavior for the Shannon entropy:

$$S_{n\to 1} = V_A \ln \mathcal{D} + \ell \ln \left[\mathcal{D}^2 \prod_{j=0}^{k} (d_j)^{-d_j^2/\mathcal{D}^2} \right] . \quad \text{(A14)}$$

APPENDIX B: RENYI ENTROPY FOR THE SU(N)$_2$ STRING-NET

Let us now briefly comment on the SU(N)$_k$ models and give the final result for the Renyi entropies of the string-net models based on the SU(N)$_2$ anyonic theories. The calculation proceeds along the same lines as in the previous appendix. Thus we only comment on the few details that differ from the previous calculation.

The SU(N)$_k$ anyonic theories have N Abelian representations. A similar calculation as the one done in Eqs. (A3) and (A4) shows that the T matrix has an N-fold degenerate, highest eigenvalue $\mathcal{D}^2$. In the SU(2)$_k$ models, we saw that the eigenvalues of the weight matrices have special properties, namely $\lambda_0^{(\beta)} = (-1)^\beta \lambda_k^{(\beta)} = d_\beta$, where 0 and k were labeling the Abelian representations. A similar property is valid for SU(N)$_k$. In order to see this let us first introduce some necessary notation. In the SU(N)$_k$ anyon theories the representations can be labeled by N component vectors $\boldsymbol{\alpha} = (\alpha_0, \ldots, \alpha_{N-1})$ [27], such that the sum of all the vector entries is k. The Abelian representations are labeled by the vectors, where one component is k and all the others are 0. For instance, we can label all the Abelian representations consecutively by vectors $\boldsymbol{\mu}_j = (\mu_{j0}, \ldots, \mu_{jN-1})$ with $j = 0, \ldots N-1$ and $\mu_{ji} = k\delta_{ji}$, where $\boldsymbol{\mu}_0 = (k, 0, \ldots, 0)$ denotes the identity representation. It can be shown by using the outer automorphism of SU(N)$_k$ that some of the eigenvalues of the weight matrices are related by phases [27]:

$$\lambda_{\boldsymbol{\mu}_j}^{(\boldsymbol{\alpha})} = \exp\left(2\pi i \sum_{s=0}^{N-1} s\alpha_s \frac{j}{N} \right) \lambda_{\boldsymbol{\mu}_0}^{(\boldsymbol{\alpha})} . \quad \text{(B1)}$$

Note that in contrast to the index $\boldsymbol{\mu}_j$, which labels an Abelian representation, $\boldsymbol{\alpha}$ may label any representation, in particular, it may label one of the non-Abelian ones. The phases are Nth roots of unity in analogy to what was found for the SU(2)$_k$ anyon theory. In analogy to the previous calculation, we can identify $\lambda_{\boldsymbol{\mu}_0}^{(\boldsymbol{\alpha})}$ with the quantum dimension of the representation labeled by $\boldsymbol{\alpha}$, i.e., $\lambda_{\boldsymbol{\mu}_0}^{(\boldsymbol{\alpha})} = d_{\boldsymbol{\alpha}}$.

The boundary weights are computed in same way as shown in Appendix A. Restricting the discussion to systems where the volumes of each of the subsystem is large and using (B1) to relate the eigenvalues of the weight matrices to the quantum dimensions, we find the following form of the boundary weights:

$$W_1(\boldsymbol{\alpha}, V) \approx \sum_{n=0}^{N-1} \exp\left(\frac{2\pi i n}{N} \sum_{j=1}^{\ell} \sum_{s=0}^{N-1} s\alpha_{js} \right) \prod_{i=1}^{\ell} d_{\boldsymbol{\alpha}_i} \mathcal{D}^V$$
$$= \begin{cases} N \prod_{i=1}^{\ell} d_{\boldsymbol{\alpha}_i} \mathcal{D}^V & \text{for } \sum_{j=1}^{\ell} \sum_{s=0}^{N-1} \frac{s\alpha_{js}}{N} \in \mathbb{N}, \\ 0 & \text{otherwise} . \end{cases} \quad \text{(B2)}$$

We note that the form of the boundary weight is very similar to what was found in Appendix A. The remaining calculation proceeds analogously to the one in Appendix A and the scaling form of the Renyi entropy—in the limit of large volumes and boundaries—looks very similar to the result of the string-net based on the SU(2)$_k$ anyon theory

$$S_n^A = V_A \ln \mathcal{D} + \ell \ln \left(\frac{\mathcal{D}^{2n}}{\mathcal{D}_{n+1}^{+}} \right)^{1/(n-1)} - (n_b - 1) \ln N , \quad \text{(B3)}$$

except that the total quantum dimension is now the one of the SU(N)$_2$ anyon theory and the topological contribution is proportional to $\ln N$, as there are N Abelian representations in SU(N)$_2$. The number of disconnected regions in subsystem B is again denoted by n_b. $\mathcal{D}_m^{\pm}$ is defined as in Eq. (A12).

APPENDIX C: EFFECTIVE LOOP MODEL

In this Appendix, we want to present an alternative description on the classical string-nets based on the SU(2)$_k$ anyon theories that is useful for understanding why the classical topological entropy is independent on the level k. The main idea is to map the SU(2)$_k$ string-nets to models of noncrossing loops, where at most k loops are allowed on each edge. The correspondence between the classical string-net and this generalized loop model is illustrated in Fig. 14 for the case of $k = 2$—the upper panel shows the allowed vertices for SU(2)$_2$ and the lower panel the corresponding vertices in the loop model. In order to reproduce the allowed vertices for SU(2)$_k$ one needs to put additional constraints on the noncrossing loop model. For instance, the loop configuration with two strings on each edge is not allowed.

The topological entropy is by definition a quantity that is not sensitive to local details. In contrast, it indicates a global conservation law, which on the classical level is enforced by local (hard) constraints. For loop models, this constraint is the

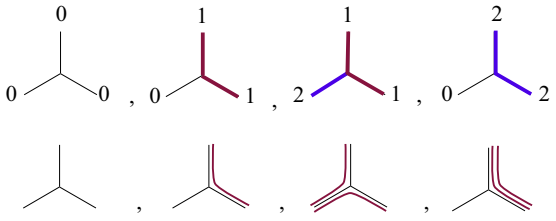

FIG. 14. (Color online) Allowed vertices up to rotation for SU(2)$_2$ string-nets using a generalized loop model. The vertices are in one-to-one correspondence to the ones in panel (b) of Fig. 4. Note that a vertex with two lines on each outgoing leg is absent in the theory.

absence of open strings. Thus, as long as the partition function contains loops on all length scales with a finite weight, the topological entropy should be given by $\ln 2$—independent of which particular loop model is studied. Thus it seems reasonable that the topological entropy of all $SU(2)_k$ models is given by $\gamma = \ln 2$.

[1] For an early review see, e.g., X.-G. Wen, Int. J. Mod. Phys. B **05**, 1641 (1991).

[2] D. C. Tsui, H. L. Stormer, and A. C. Gossard, Phys. Rev. Lett. **48**, 1559 (1982).

[3] Y. Maeno, H. Hashimoto, K. Yoshida, S. Nishizaki, T. Fujita, J. G. Bednorz, and F. Lichtenberg, Nature (London) **372**, 532 (1994).

[4] C. L. Kane and E. J. Mele, Phys. Rev. Lett. **95**, 226801 (2005).

[5] A. Kitaev, Ann. Phys. **303**, 2 (2003).

[6] A. Kitaev, Ann. Phys. **321**, 2 (2006).

[7] X. Chen, Z.-C. Gu, and X.-G. Wen, Phys. Rev. B **82**, 155138 (2010).

[8] X. Chen, Z.-C. Gu, Z.-X. Liu, and X.-G. Wen, Phys. Rev. B **87**, 155114 (2013).

[9] A. Kitaev and J. Preskill, Phys. Rev. Lett. **96**, 110404 (2006).

[10] M. Levin and X. G. Wen, Phys. Rev. Lett. **96**, 110405 (2006).

[11] S. T. Flammia, A. Hamma, T. L. Hughes, and X. G. Wen, Phys. Rev. Lett. **103**, 261601 (2009).

[12] S. H. Simon and P. Fendley, J. Phys. A **46**, 105002 (2013).

[13] C. Castelnovo and C. Chamon, Phys. Rev. B **76**, 174416 (2007).

[14] There are also generalizations of entanglement measures where the system is divided into multiple ($\geqslant 2$) partitions, such as analysed in R. Orús, T.-C. Wei, O. Buerschaper, and M. Van den Nest, New J. Phys. **16**, 013015 (2014).

[15] R. G. Melko, A. B. Kallin, and M. B. Hastings, Phys. Rev. B **82**, 100409 (2010).

[16] J. Iaconis, S. Inglis, A. B. Kallin, and R. G. Melko, Phys. Rev. B **87**, 195134 (2013).

[17] H.-C. Jiang, Z. Wang, and L. Balents, Nat. Phys. **8**, 902 (2012).

[18] S. Depenbrock, I. P. McCulloch, and U. Schollwöck, Phys. Rev. Lett. **109**, 067201 (2012).

[19] M. A. Levin and X.-G. Wen, Phys. Rev. B **71**, 045110 (2005).

[20] V. G. Drinfeld, *Proceedings of the International Congress of Mathematicians 1986* (American Mathematical Society, Providence, RI, 1987), Vol. 1, pp. 798–820.

[21] C. Gils, S. Trebst, A. Kitaev, A. Ludwig, M. Troyer, and Z. Wang, Nat. Phys. **5**, 834 (2009).

[22] For a more mathematical introduction the reader is referred to the early chapters of Z. Wang, *Topological Quantum Computation*, Conference Board of the Mathematical Sciences (American Mathematical Society, Providence, RI, 2010), Vol. 112.

[23] In even more general terms, a representation is called non-Abelian if fused with any other representation of the same anyonic theory leads to more than one fusion outcome.

[24] M. Müger, J. Pure Appl. Algebra **180**, 159 (2003).

[25] Note the subtle difference to the loop gas configurations of the toric code model, which are equal-weight superpositions of closed loop configurations, similar to those occurring for the $SU(2)_1$ anyon theory, where all coefficients a_s are strictly positive and of identical magnitude.

[26] A. Rahmani and G.-W. Chern, Phys. Rev. B **88**, 054426 (2013).

[27] P. Di Francesco, P. Mathieu, and D. Sénéchal, *Conformal Field Theory* (Springer, New York 1997).